ANL/CSE-14/35

Peroxide Formation, Destruction, and Precipitation in Uranyl Sulfate Solutions: Simple Addition and Radiolytically Induced Formation

Chemical Sciences and Engineering Division

About Argonne National Laboratory
Argonne is a U.S. Department of Energy laboratory managed by UChicago Argonne, LLC under contract DE-AC02-06CH11357. The Laboratory's main facility is outside Chicago, at 9700 South Cass Avenue, Argonne, Illinois 60439. For information about Argonne and its pioneering science and technology programs, see www.anl.gov.

DOCUMENT AVAILABILITY

Online Access: U.S. Department of Energy (DOE) reports produced after 1991 and a growing number of pre-1991 documents are available free via DOE's SciTech Connect (http://www.osti.gov/scitech/).

Reports not in digital format may be purchased by the public from the National Technical Information Service (NTIS):

U.S. Department of Commerce
National Technical Information Service
5301 Shawnee Rd
Alexandria, VA 22312
www.ntis.gov
Phone: (800) 553-NTIS (6847) or (703) 605-6000
Fax: (703) 605-6900
Email: **orders@ntis.gov**

Reports not in digital format are available to DOE and DOE contractors from the Office of Scientific and Technical Information (OSTI):

U.S. Department of Energy
Office of Scientific and Technical Information
P.O. Box 62
Oak Ridge, TN 37831-0062
www.osti.gov
Phone: (865) 576-8401
Fax: (865) 576-5728
Email: **reports@osti.gov**

Disclaimer
This report was prepared as an account of work sponsored by an agency of the United States Government. Neither the United States Government nor any agency thereof, nor UChicago Argonne, LLC, nor any of their employees or officers, makes any warranty, express or implied, or assumes any legal liability or responsibility for the accuracy, completeness, or usefulness of any information, apparatus, product, or process disclosed, or represents that its use would not infringe privately owned rights. Reference herein to any specific commercial product, process, or service by trade name, trademark, manufacturer, or otherwise, does not necessarily constitute or imply its endorsement, recommendation, or favoring by the United States Government or any agency thereof. The views and opinions of document authors expressed herein do not necessarily state or reflect those of the United States Government or any agency thereof, Argonne National Laboratory, or UChicago Argonne, LLC.

ANL/CSE-14/35

Peroxide Formation, Destruction, and Precipitation in Uranyl Sulfate Solutions: Simple Addition and Radiolytically Induced Formation

by
Amanda J. Youker, James Jerden, Michael Kalensky, Kevin Quigley,
Charles Jonah, Sergey Chemerisov, and George F. Vandegrift
Chemical Sciences and Engineering Division, Argonne National Laboratory

prepared for
U.S. Department of Energy, National Nuclear Security Administration,
Office of Defense Nuclear Nonproliferation

October 2014

CONTENTS

ABSTRACT 1

1 INTRODUCTION 2

1.1 Bench-Top Experiments 2
1.2 Van de Graaff Experiments 4

2 EXPERIMENTAL 5

2.1 Bench-Top Experiments 5
2.2 Van de Graaff Experiments 6

3 RESULTS AND DISCUSSION 7

3.1 Bench-Top Experiments 7
3.2 Preliminary Kinetic Model for the Catalytic Destruction of H_2O_2 11
3.2.1 Purpose 11
3.2.2 Method 11
3.2.3 Model System 12
3.2.4 Results and Discussion of Model 13
3.3 Van de Graaff Results 16
3.3.1 Samples 1 and 2 16
3.3.2 Sample 3 18
3.3.3 Samples 4-7 18

4 CONCLUSIONS 26

4.1 Bench-Top Experiments 26
4.2 Model Development 27
4.3 Van de Graaff Experiments 27

5 REFERENCES 28

FIGURES

1 Variations of the Radiolytic Yield of the Dominant Radicals and Molecular Species Produced during Irradiation of an Acidic Sulfate Solution 3

2 Photographs of Typical Titration Test Samples and Typical XRD Results from Precipitate 7

FIGURES (Cont.)

3 Photographs of Typical Titration Test Samples Containing an Initial Concentration of Ferrous Iron 8

4 Data from Titration Tests Measuring the Amount of H_2O_2 Required to Achieve Precipitation Over a Range of Relevant Conditions 9

5 Results from Titration Tests and Thermodynamic Saturation State Modeling 10

6 Data from a Uranyl Sulfate Solution Reactor Study Used to Estimate Parameter Values for the Thermodynamic/Kinetic Model 11

7 Results from Titration Experiments and the Thermodynamic/Kinetic Model Showing How Different Concentrations of Iron can Influence the Saturation State of a 110 g-U/L Uranyl Sulfate Solution to which H_2O_2 is Added at a Constant Rate 13

8 Results from the Thermodynamic/Kinetic Model Showing How the Thermal Decomposition of H_2O_2 Determines the Steady-State Concentration of H_2O_2 for a Constant Titration Rate of 7 μmoles per Kilogram Solution per Second 14

9 Results from the Thermodynamic/Kinetic Model Showing How the Interplay of Fe(II) Oxidation and the Rate of Fe(III) Reduction Determines the Steady-State Concentration of H_2O_2 for a Constant Titration Rate of 7 μmoles per Kilograms Solution per Second 15

10 H_2 and O_2 Produced as a Function of Dose for Sample 1 19

11 H_2-to-O_2 Ratio as a Function of Dose for Sample 1 19

12 H_2 and O_2 Produced as a Function of Dose for Sample 2 20

13 H_2-to-O_2 Ratio as a Function of Dose for Sample 2 20

14 H_2 and O_2 Produced as a Function of Dose for Sample 3 21

15 H_2-to-O_2 Ratio as a Function of Dose for Sample 3 21

16 H_2 and O_2 Produced as a Function of Dose for Sample 4 22

17 H_2-to-O_2 Ratio as a Function of Dose for Sample 4 22

18 H_2 and O_2 Produced as a Function of Dose for Sample 5 23

FIGURES (Cont.)

19 H_2-to-O_2 Ratio as a Function of Dose for Sample 5 23

20 H_2 and O_2 Produced as a Function of Dose for Sample 6..... 24

21 H_2-to-O_2 Ratio as a Function of Dose for Sample 6 24

22 H_2 and O_2 Produced as a Function of Dose for Sample 7..... 25

23 H_2-to-O_2 Ratio as a Function of Dose for Sample 7 25

TABLES

1 Van de Graaff Irradiation Results for Uranyl Sulfate Solutions..... 17

2 G Values for Hydrogen and Oxygen 18

This page intentionally left blank

PEROXIDE FORMATION, DESTRUCTION, AND PRECIPITATION IN URANYL SULFATE SOLUTIONS: SIMPLE ADDITION AND RADIOLYTICALLY INDUCED FORMATION

ABSTRACT

SHINE Medical Technologies plans to use fissioning of a low enriched uranium (LEU) solution as uranyl sulfate for molybdenum-99 production. One of the major concerns for SHINE is peroxide formation from radiolysis, which can lead to precipitation of uranyl peroxide. Bench-top experiments where peroxide was added directly to a uranyl sulfate solution were performed to determine the concentration where precipitation occurs as a function of temperature and concentration of ferrous or ferric ion to aid in peroxide destruction. Based on the experimental results and relevant literature, a thermodynamic/kinetic model for the precipitation of uranyl peroxide for a given set of conditions was developed and tested. The conditions that must be specified in the model are temperature, uranyl sulfate concentration, ferrous- or ferric-ion concentration, and the H_2O_2 production rate. Additionally, experiments were performed using the Van de Graaff accelerator as a radiation source for radiolytically induced peroxide formation. Uranyl peroxide precipitated at 12°C when a uranyl sulfate solution was exposed to a radiation dose of 7900 Mrad in the pulse mode, but precipitation did not occur in the direct current (DC) mode at much higher powers. Because precipitation could not be achieved in the DC mode for this set of experiments, the effects of temperature and power on uranyl peroxide formation could not be determined. Future experiments will monitor current continuously, measure gas flow rates continuously, and use a uranyl sulfate solution that contains little to no iron impurity.

1 INTRODUCTION

In the fissioning of an LEU solution as uranyl sulfate for production of Mo-99 to be used in medical applications, peroxide formation from radiolysis can lead to precipitation of uranyl peroxide [1]. Work on aqueous homogenous reactors with uranyl sulfate fuel in the 1950s showed that the reactor power is limited by the concentration of peroxide produced by fission fragments in solution [2, 3]. The concentration of radiolytic peroxide increases as the power density increases until the fuel solution becomes saturated with respect to uranyl peroxide. The solubility product of uranyl peroxide helps to determine a threshold power density above which the fuel precipitates, causing off-normal operating conditions.

The precipitation of uranyl peroxide is also a concern in subcritical uranyl sulfate target solutions that are bombarded with neutrons to produce the Mo-99. The following study provides information on uranyl peroxide precipitation from uranyl sulfate in support of the development of a solution-based means of Mo-99 production. Both bench-top and 3 MeV Van de Graaff accelerator experiments were undertaken.

1.1 BENCH-TOP EXPERIMENTS

The three objectives of the bench-top experiments were to (1) quantify the solubility product of uranyl peroxide and determine how it varies with temperature, (2) quantify how the presence of ferrous and ferric iron in solution delays or inhibits the precipitation of uranyl peroxide due to the enhanced destruction of aqueous peroxide, and (3) develop a preliminary kinetic model that could be used to predict the onset of uranyl peroxide precipitation for a given set of conditions (H_2O_2 production rate, temperature, Fe^{2+}/Fe^{3+} concentration(s), and uranium concentration).

The experiments involved titrating a uranyl sulfate solution with known amounts of hydrogen peroxide at a controlled rate. This approach is a simple simulation of an aqueous target solution, where the addition of peroxide will be determined by the dose rate and the radiolytic yield of peroxide. Figure 1 provides the context for the titration experiments, as well as ongoing experiments being performed at Argonne's Low Energy Accelerator Facility. It shows that the generation rate or radiolytic yield values for hydrogen peroxide and hydrogen, as well as the important radicals H^-, OH^-, and HO_2, depend on the linear energy transfer (LET) of the particles causing radiolysis. Tests performed with low-LET radiation, such as the Van de Graaff irradiation experiments (Section 1.2), will produce relatively high levels of H^- and OH^- radicals, which can influence the generation rate of peroxide. With high-LET bombardment typical of a target solution undergoing fission, the non-molecular radicals are insignificant, but the primary yields of both hydrogen peroxide and hydrogen increase relative to low-LET particles. These types of details are being accounted for in Argonne's experiments, so the results can be scaled to provide information relevant to production-level methods for Mo-99 generation.

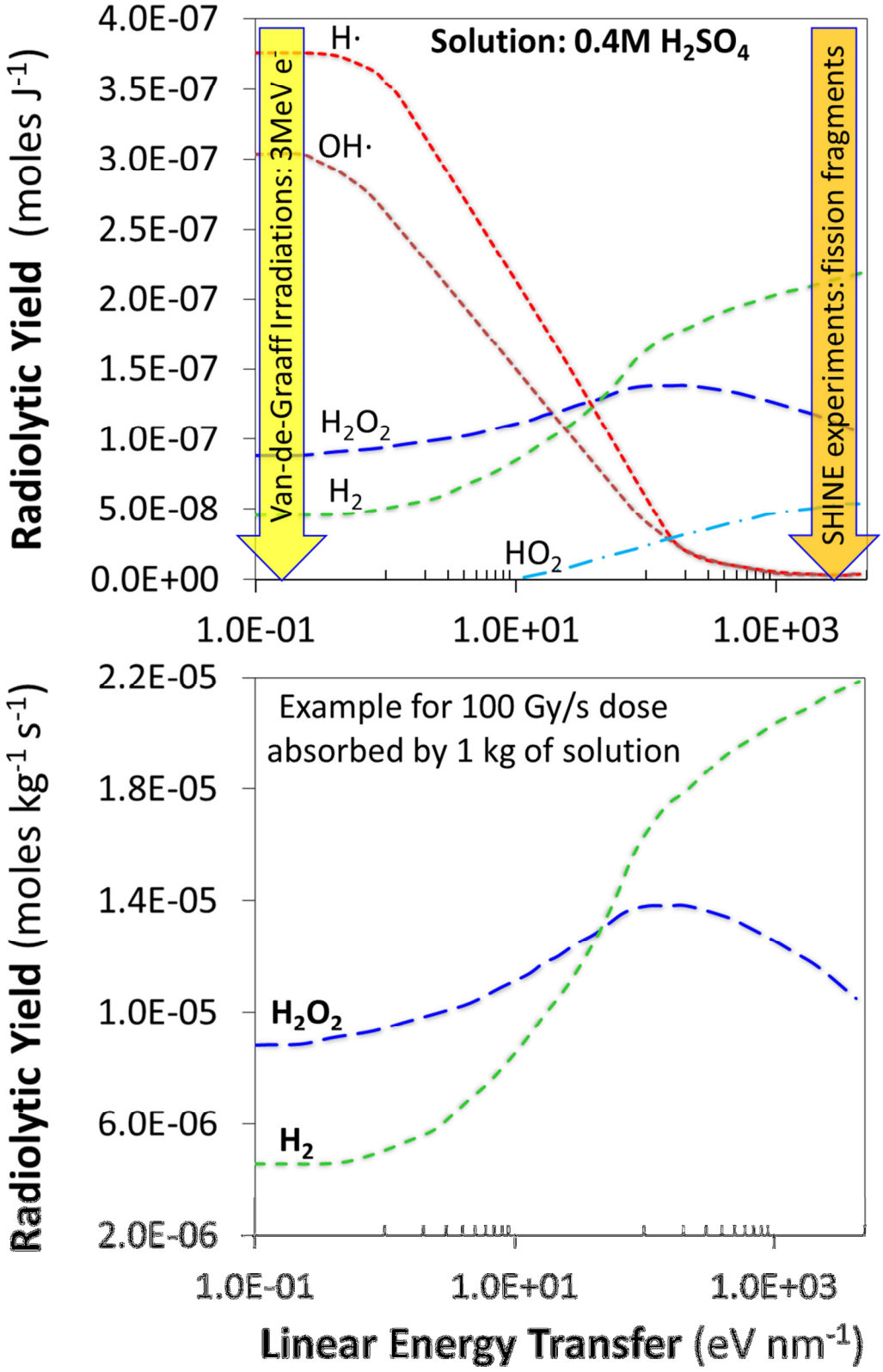

FIGURE 1 Variations of the Radiolytic Yield of the Dominant Radicals and Molecular Species Produced during Irradiation of an Acidic Sulfate Solution [4]

1.2 VAN DE GRAAFF EXPERIMENTS

Argonne's 3 MeV Van de Graaff accelerator was used as a source of radiation to examine the formation of peroxide in a uranyl sulfate solution and possible precipitation of uranyl peroxide. Doses equivalent to 5,500-32,500 Mrad were applied to a uranyl sulfate solution, and the temperature was controlled at 12-34°C. About 70 ppm Fe was already present in the solution as an impurity in the depleted uranium foils used to prepare the uranyl sulfate solution. A second uranyl sulfate solution was prepared from depleted uranium plates, and approximately 10 ppm Fe was present in the solution. This iron was most likely due to leaching from the stainless steel beakers used in the preparation of the stock solution.

These experiments were performed to gain a better understanding of the effects of temperature and iron concentration on peroxide formation and uranyl peroxide precipitation. Solutions were analyzed approximately 15-20 min post-irradiation to determine the concentration of peroxide in solution and the amount of uranium that precipitated as uranyl peroxide when a precipitate was observed. Additionally, the formation of hydrogen and oxygen was measured with a residual gas analyzer (RGA) during each irradiation.

2 EXPERIMENTAL

2.1 BENCH-TOP EXPERIMENTS

A uranyl sulfate solution (pH 1) of 110 g-U/L was prepared by dissolving uranium foils in a sulfuric acid/hydrogen peroxide mixture. The uranium concentration was confirmed by inductively coupled plasma/optical emission spectroscopy (ICP-OES), and the pH was measured before and after each experiment.

Titrations were performed in 10 mL Pyrex beakers. For each test, two grams of the 110 g-U/L solution was added to a beaker, and the pH was monitored. The temperature was varied from room temperature to 80°C by using a hot plate and an aluminum "well," where the beaker was held during experiments. The aluminum well was heated to ensure that the sides of the beaker were the same temperature as the hot plate. A 30% hydrogen peroxide solution was diluted to 0.01 mol/kg just prior to the experiments and used as the titrant.

In early experiments, a turbidity meter was used to determine the onset of precipitation. However, due to very rapid precipitation kinetics, it was found that the experimenter's eyes were just as sensitive as the meter for determining the onset of stable crystal growth.

The titration was performed using a micropipette, and all tests were run with a steady titration rate of 7 micromoles of H_2O_2 per liter per second. The final solution concentrations were all corrected for dilution.

A number of titrations were continued past the inception of precipitation, so that enough precipitate could be collected for powder X-ray diffraction (XRD) analyses. These samples were centrifuged and washed three times with deionized water to remove uranyl sulfate residue prior to drying and XRD analyses.

Uranyl peroxide precipitation tests were performed at temperatures of 20°C, 40°C, 50°C, 60°C, 70°C, and 80°C. The temperature of the solution was measured with a J-type thermocouple. Results from the 70°C and 80°C tests are questionable because it appears that the experimental setup was not adequately adiabatic; that is, the heat loss from the solution surface caused temperature fluctuations in the solution (the thermocouple reading did not stabilize during titration).

The effect of ferrous and ferric iron on the titration tests was quantified by running a set of experiments at 40°C in which iron was added to the 110 g-U/L uranyl sulfate solution. The ferrous iron test solutions contained 0.001 to 0.01 mol/kg Fe(II) (added as ferrous sulfate). The effect of ferric iron was tested by adding excess ferric oxyhydroxide to the solution.

2.2 VAN DE GRAAFF EXPERIMENTS

Argonne's 3 MeV Van de Graaff accelerator was used as a source of high radiation dose rates to generate peroxide in uranyl sulfate solutions. The doses applied to the solution were determined by using oxalic acid as a dosimeter [5]. During the first three experiments, 2 mL of a uranyl sulfate solution with 163 g-U/L was irradiated for 3-10 hours at a current of 5 μA. A new solution containing 115 g-U/L uranyl sulfate was used for the final four experiments, where irradiation times were 5-10 hours at currents between 10 and 20 μA. The temperature was controlled at 12-29°C by means of a water bath, and gases were analyzed with an RGA and helium cover gas. The solutions were not deaerated before irradiation. The seven samples were irradiated in the pulse and DC mode with doses applied to each sample ranging from 5,500 to 32,500 Mrad.

Samples were analyzed approximately 20 min post-irradiation using an indirect means of analysis that measures the decrease in absorbance at 628 nm for toluidine blue [6]. An aliquot of the irradiated solution (100-500 μL) was contacted with an excess of potassium iodide in the presence of hydrochloric acid, toluidine blue, and sodium acetate. If peroxide is present in solution, it oxidizes the iodide to iodine, while bleaching the toluidine blue in acidic solution. The amount of free iodine is directly proportional to the peroxide concentration in solution. If a precipitate was observed, the solution was centrifuged, and an aliquot of the remaining liquid was submitted for ICP-OES analysis to determine the amount of uranyl peroxide that precipitated under each set of conditions.

3 RESULTS AND DISCUSSION

3.1 BENCH-TOP EXPERIMENTS

Figures 2 (top) shows before and after photographs of a typical titration experiment. The precipitate was clearly identified by XRD (Figure 2, bottom) as the uranyl peroxide mineral metastudtite (UO_4•$2H_2O$).

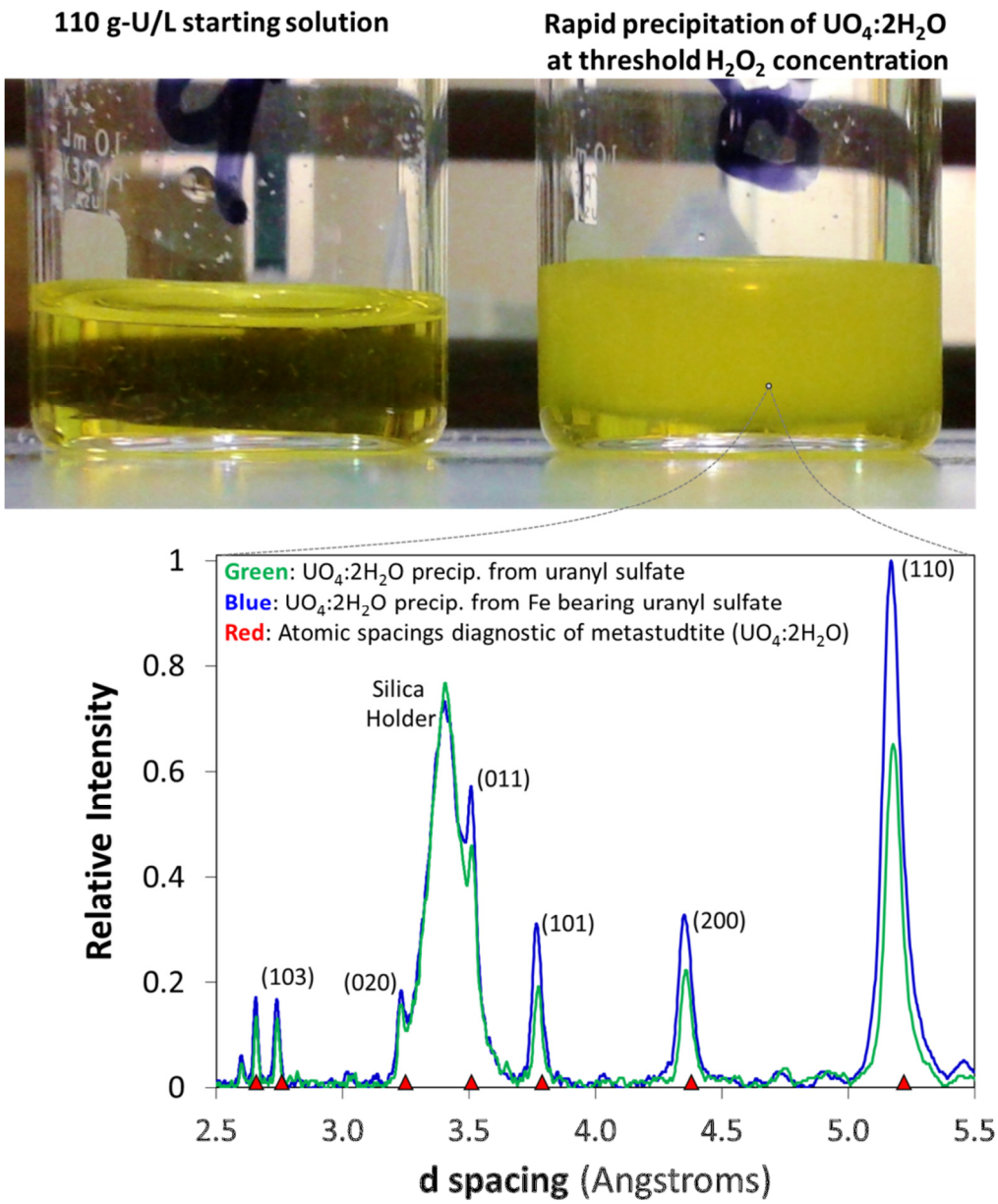

FIGURE 2 Photographs of Typical Titration Test Samples (top) and Typical XRD Results from Precipitate (bottom). Note the purity and crystallinity of the solid produced.

The titrations performed on uranyl sulfate solutions containing ferrous iron resulted in a gradual darkening and orange color shift, as shown in Figure 3. The color shift is due to the rapid oxidation of Fe(II) to Fe(III) by H_2O_2. Visual observations suggest that, as Fe(III) is formed, the destruction of H_2O_2 leads to the formation of O_2 gas bubbles (Figure 3). The pH for all titration tests was fairly constant within a range of 0.9-1.2 (accounting for temperature effect). There was no obvious trend in pH variations.

Results from the titration experiments yield insight into both the solubility of $UO_4 \bullet 2H_2O$ and the rate of peroxide decomposition due to increased temperature and the presence of iron. The amount of H_2O_2 required to achieve precipitation under different conditions is shown in Figure 4. Each data point is for a single titration. The amount of H_2O_2 required to achieve

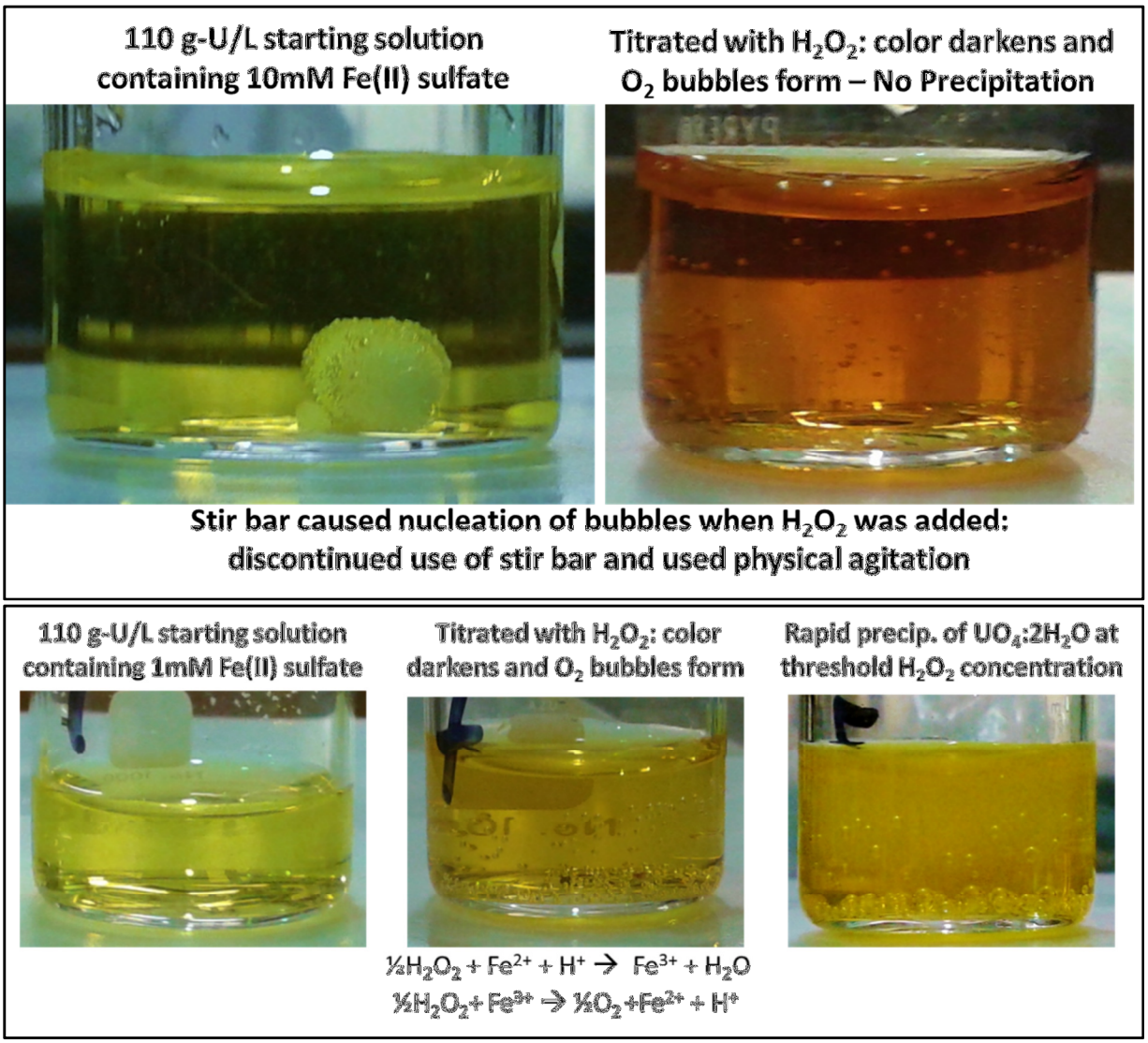

FIGURE 3 Photographs of Typical Titration Test Samples Containing an Initial Concentration of Ferrous Iron

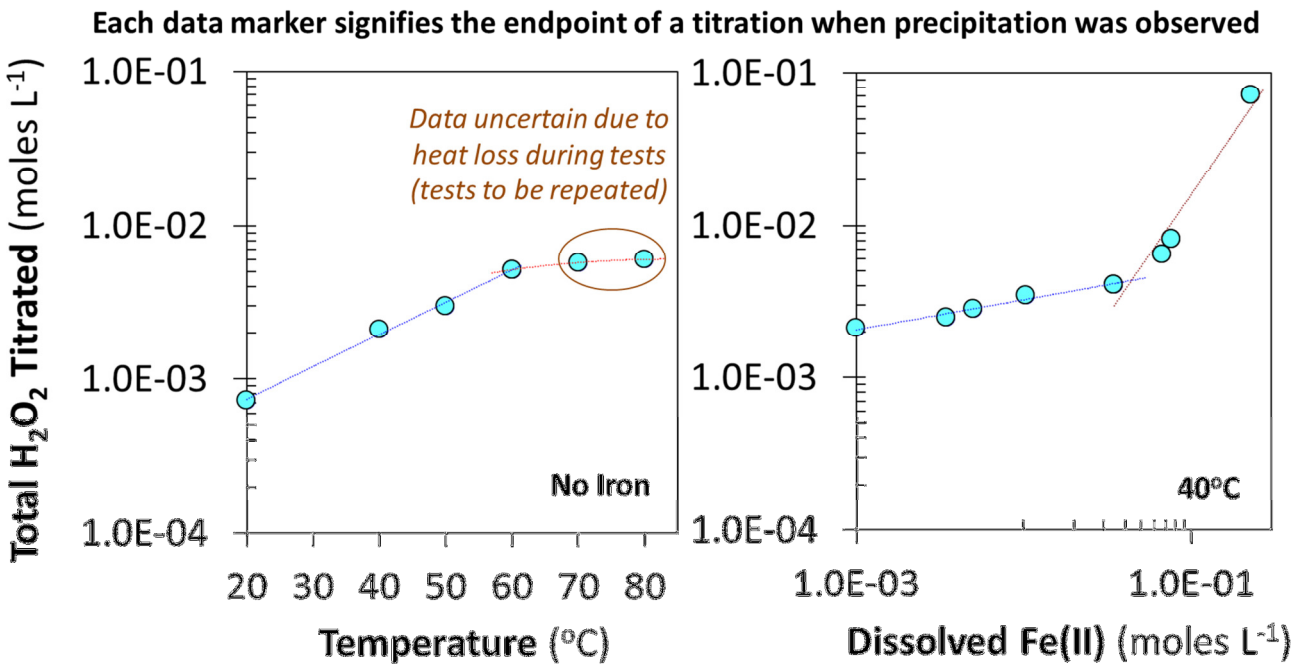

FIGURE 4 Data from Titration Tests Measuring the Amount of H_2O_2 Required to Achieve Precipitation Over a Range of Relevant Conditions. Solution is 110 g/L uranyl sulfate at pH = 1, and the titration rate was 7 µmoles per kilogram solution per second.

precipitation increases with increasing temperature (Figure 4, left) and increasing Fe(II) concentration (Figure 4, right). This is because the rates of thermal decomposition and oxidation of iron by H_2O_2 are comparable to the titration rate: 7 micromoles H_2O_2 per kg of solution per second. Some fraction of H_2O_2 is being destroyed during the titration, thus increasing the amount of titrant needed to reach the precipitation threshold concentration.

As mentioned above, the points at 70°C and 80°C are questionable due to unstable solution temperature readings during these tests. Heat loss from the surface of the solution may have resulted in the actual temperatures being 5 to 8 degrees lower than what is shown in Figure 4.

The presence of ferric iron, both dissolved and as a granular powder of goethite, did not delay the onset of precipitation for a given temperature. This observation suggests that the rate of reduction of Fe(III) by H_2O_2 is low relative to the titration rate.

Because of the rapidity of $UO_4 \bullet 2H_2O$ precipitation (even at 20°C), the measured data can be used to confirm the solubility product of the precipitate. Our results are in agreement with previous qualitative observations that the solubility of uranyl peroxide in ~100 g-U/L uranyl sulfate is around 1 mM H_2O_2 [1]. Figure 5 compares our titration method results with the solubility product (K_{sp}) of metastudtite that is commonly used in thermodynamic databases (we used "data0.ymp.R5" of Wolery and Jove-Colon [7]).

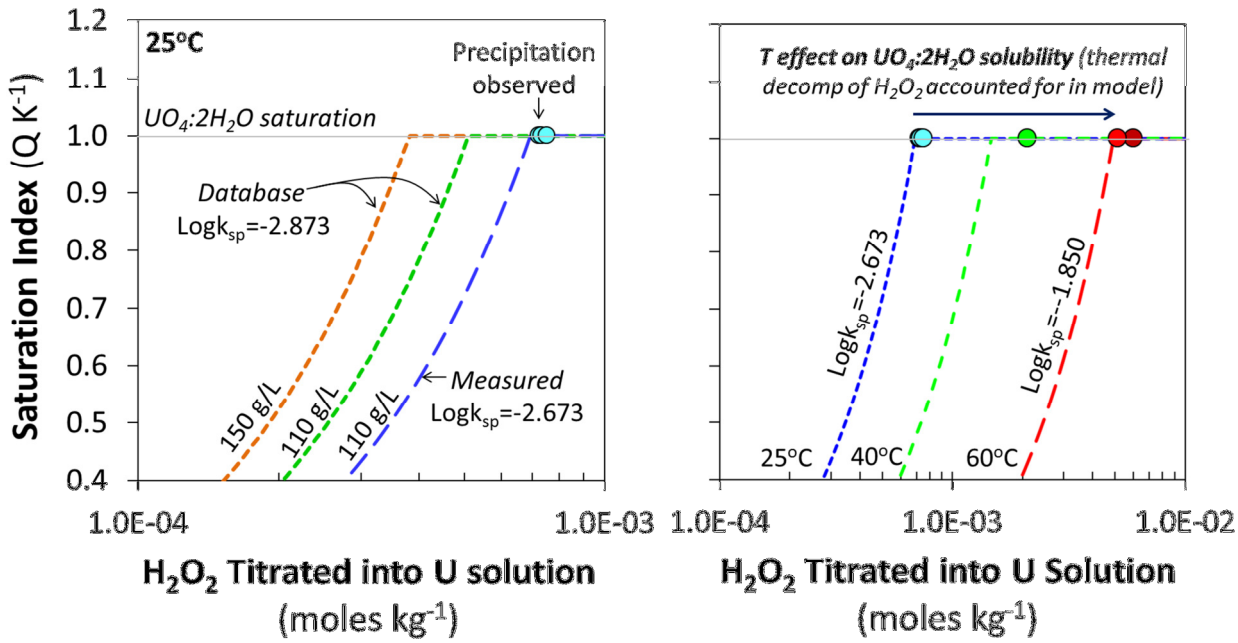

FIGURE 5 Results from Titration Tests (data points) and Thermodynamic Saturation State Modeling (dotted lines)

The saturation index plots shown in Figure 5 were made with the thermodynamic/kinetic reaction path code "The Geochemist's Workbench®", Professional Release 8.0 (GWB). The saturation state calculations (dotted lines) are for a uranyl sulfate solution of 110 g-U/L at pH 1.

The K_{sp} for uranyl peroxide measured in the titration experiments is around 1.6 times higher than the value used in the data0.ymp.R5 database. This relatively small discrepancy could be explained by either (1) the decomposition of peroxide prior to precipitation (the titration concentration is the total added and does not account for H_2O_2 lost during titration) or (2) a relatively small activation energy barrier associated with mineral nucleation that must be overcome once the solubility product is exceeded.

However, recently reported solubility measurements made on metastudtite ($UO_4 \bullet 4H_2O$) using an undersaturation approach agree (within error) with the value extracted from our titration results: Giménez et al. measured a $\log K_{sp}$ of -2.7±0.2, while the value from the titration tests is -2.67 [8]. This agreement indicates that the titration method is accurate and suggests that there is no significant activation energy for precipitating uranyl peroxide, even at room temperature.

The temperature dependence of the solubility product of uranyl peroxide can also be extracted from the titration test data (Figure 5, right). Based on the measured rate of thermal decomposition of H_2O_2 in uranyl sulfate (Figure 6, adapted from Silverman et al. [3]), we can account for the amount of peroxide lost during elevated temperature titrations. This allowed us to quantify how the K_{sp} of the metastudtite precipitate changes from 25°C to 60°C (Figure 5).

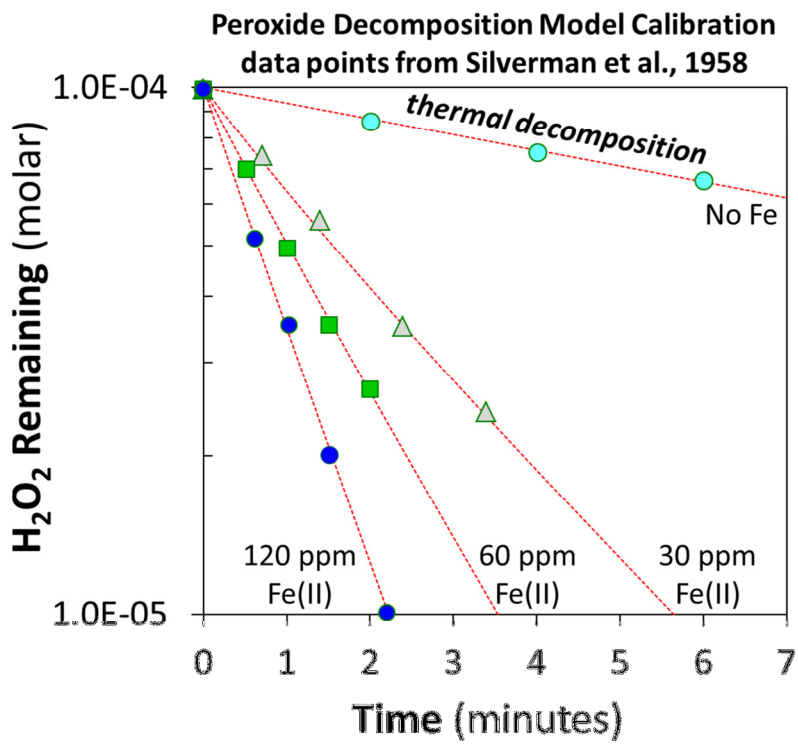

FIGURE 6 Data from a Uranyl Sulfate Solution Reactor Study [3] Used to Estimate Parameter Values for the Thermodynamic/Kinetic Model

3.2 PRELIMINARY KINETIC MODEL FOR THE CATALYTIC DESTRUCTION OF H_2O_2

3.2.1 Purpose

The purpose of this effort was to develop a tool for calculating a steady-state concentration of hydrogen peroxide for a known production rate and known temperature and reagent concentration. The steady-state concentration of hydrogen peroxide will determine whether uranyl peroxide precipitates. The calculation tool was developed with a Gibb's free energy minimization reaction path code (GWB) in which the key reactions were restricted by kinetic expressions.

3.2.2 Method

The model is not mechanistic, but is meant to capture the overall kinetic balance of the key redox reactions and allow sensitivity analyses. If the model can be "calibrated" by using literature and experimentally determined rate descriptions, it could be a useful tool for interpreting test results and prioritizing new experiments.

The key reactions that are described by rate laws are:

$$H_2O_2 \rightarrow 0.5\ O_2(aq) + H_2O \quad (1)$$

$$Fe^{3+} + 0.5H_2O_2 \rightarrow Fe^{2+} + 0.5\ O_2(aq) + H^+ \quad (2)$$

$$Fe^{2+} + 0.5H_2O_2 + H^+ \rightarrow Fe^{3+} + H_2O \quad (3)$$

$$Fe^{2+} + 0.25\ O_2(aq) + H^+ \rightarrow Fe^{3+} + 0.5\ H_2O \quad (4)$$

A traditional collision theory rate expression was used for all four reactions:

$$r_{\vec{k}} = n_w\ k_+ \prod_j (a_j \mid m_j)^{P_j} \quad (5)$$

where n_w is the mass of solvent water (kg), and k_+ is the intrinsic rate constant (expressed in molal per second). The product function Π in this equation accounts for the reactant and the promoting and inhibiting species j in the rate law; the activity or molality of each such species is raised to the power P_j. Each of these species may be an aqueous species, mineral, surface species (in which case it is represented by its molality), gas (by fugacity), or the solvent (by activity).

The rate constant is defined by the following Arrhenius relationship:

$$k_+ = A\ e^{-E_A/RT_K} \quad (6)$$

where A is the pre-exponential frequency factor, E_A is the activation energy, R is the gas constant, and T is the temperature in kelvin.

For this initial implementation of the model, the following rate constant equations were used for reactions 1 – 4, respectively:

$$k_+ = 4.0E{+}12\ (s^{-1})\exp[-105\ (kJ/mol)/RT] \quad (7)$$

$$k_+ = 2.5E{+}6\ (s^{-1})\exp[-35\ (kJ/mol)/RT] \quad (8)$$

$$k_+ = 1.0E{+}5\ (s^{-1})\exp[-35\ (kJ/mol)/RT] \quad (9)$$

$$k_+ = 1.0E{+}3\ (s^{-1})\exp[-35(kJ/mol)/RT] \quad (10)$$

All of these rate constants were extracted from the data of Silverman et al. [3] (see Figure 6) except for equation (10), which is from Stumm and Lee [9].

3.2.3 Model System

The model system included 1 kg of uranyl sulfate with 0.5 molal uranium and 0.62 molal sulfate. The starting pH was 1.0. Speciation reactions such as the formation of uranyl sulfate and

ferrous and ferric sulfate complexes were not restricted by kinetics (they are in equilibrium at every time step). The temperature and the amount of iron were varied. The addition or formation rate of H_2O_2 was set at 7.0 µmol/s to match the titration rate of the experiments described in Section 3.1.

3.2.4 Results and Discussion of Model

The model allows us to predict when uranyl peroxide will precipitate during a titration given a constant rate of addition of H_2O_2 and a known concentration of ferrous iron and constant temperature. Examples of this type of calculation are shown in Figure 7.

As shown in Figure 7 the amount of H_2O_2 required to saturate the solution with respect to $UO_4 \bullet 2H_2O$ increases by a factor of 3.5 over a range of 1-10 mM Fe(II). This implies that around 5 millimoles of H_2O_2 is reduced by Fe(II) during the course of titration. These results imply that the reaction of ferric iron with H_2O_2 (reaction 3) is slow relative to the titration rate. For the case shown in Figure 7 (110 g-U/L uranyl sulfate, 25°C, 7 µmol H_2O_2 /kg/s), the model predicts that 50 mM Fe(II) is enough to inhibit the precipitation of $UO_4 \bullet 2H_2O$. This precipitation occurs

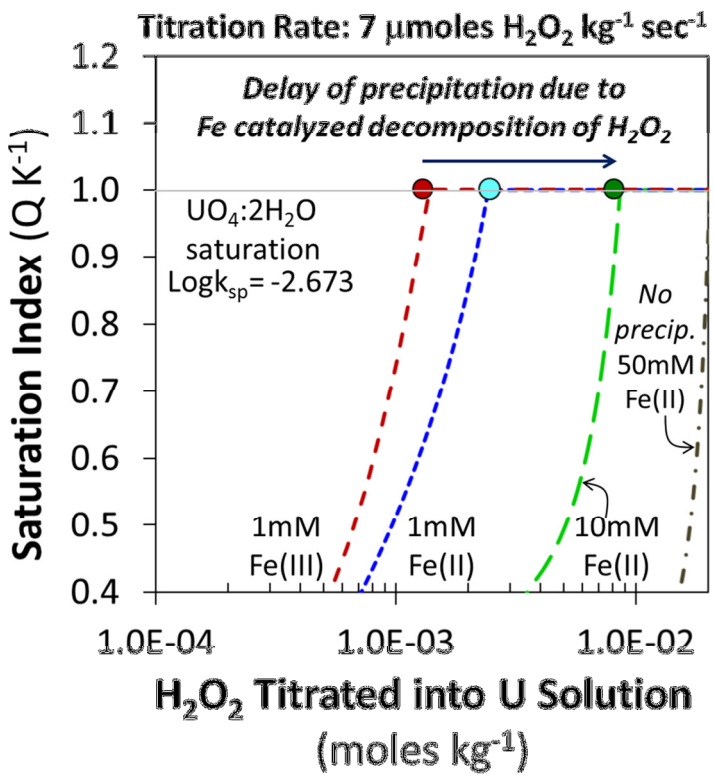

FIGURE 7 Results from Titration Experiments (points) and the Thermodynamic/Kinetic Model (lines) Showing How Different Concentrations of Iron can Influence the Saturation State of a 110 g-U/L Uranyl Sulfate Solution to which H_2O_2 is Added at a Constant Rate

because the final steady-state concentration of H_2O_2 falls below the saturation concentration for these conditions.

The key variable predicted by the model is the steady-state concentration of H_2O_2 established by the interplay of reactions 1–4. Figure 8 shows results from a series of model runs focused on the steady-state concentration of H_2O_2 at different temperatures in the absence of iron. The model predicts that steady state is established by the relative rates of thermal decomposition and the constant titration or production rate of H_2O_2.

The key observation from Figure 8 is how sensitive the thermal decomposition rate is to temperature. The model predicts that at 80°C the H_2O_2 steady-state concentration falls below the uranyl-peroxide saturation concentration. However, a temperature drop of only 5°C leads to a H_2O_2 concentration above the saturation point, and precipitation is predicted to ensue. At even lower temperatures, a considerable amount of uranyl peroxide is predicted to precipitate (around

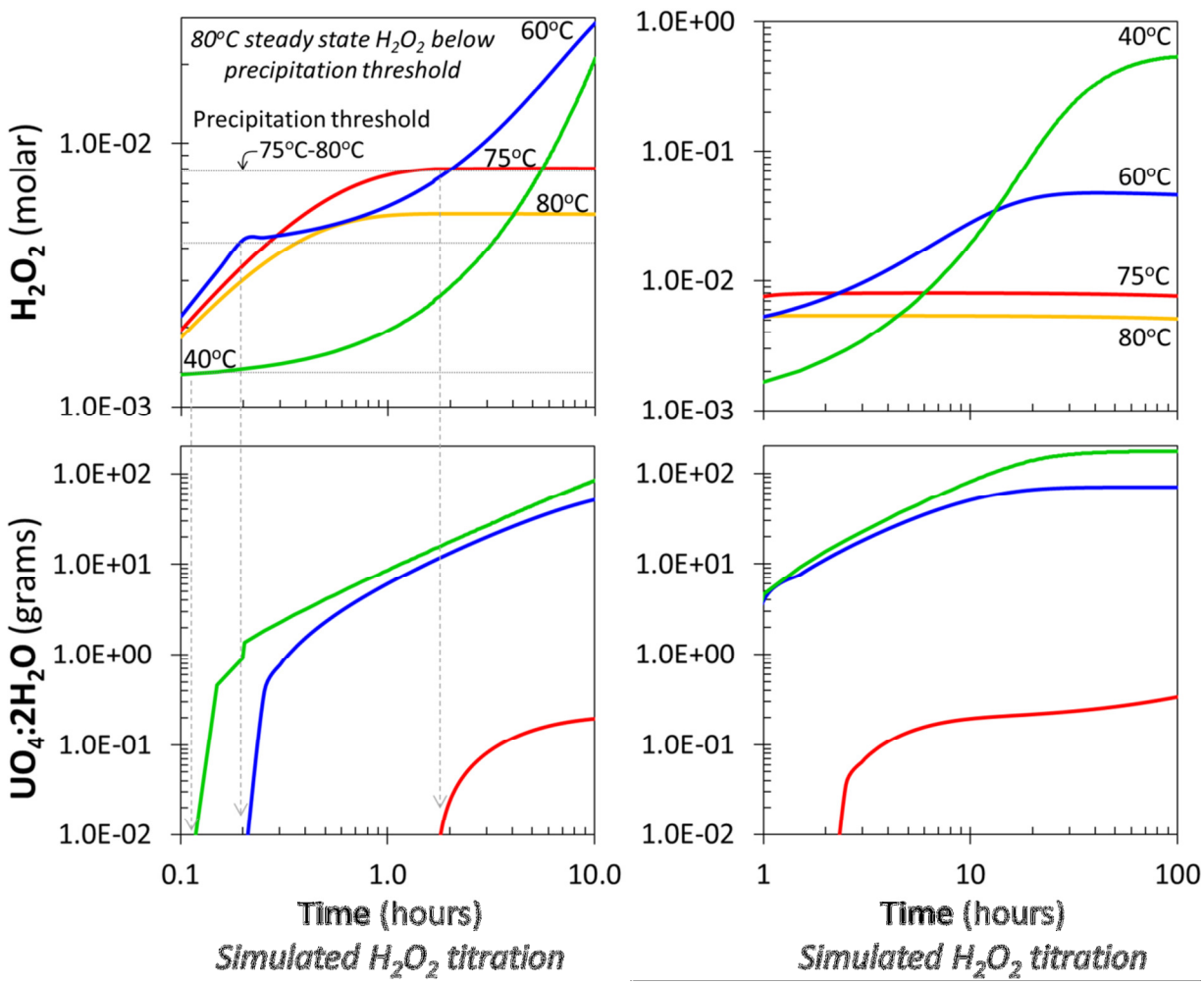

FIGURE 8 Results from the Thermodynamic/Kinetic Model Showing How the Thermal Decomposition of H_2O_2 Determines the Steady-State Concentration of H_2O_2 for a Constant Titration Rate of 7 μmoles per Kilogram Solution per Second (110 g-U/L uranyl sulfate at pH = 1)

90% of the uranium for the 40°C case). The lower right plot of Figure 8 shows that the system requires approximately 30 h to reach steady state for temperatures less than 60°C, but only 8 h for temperatures greater than 70°C.

Figure 9 shows results from a series of model runs in which ferrous iron is present at a starting concentration of 10 mM. The results show how sensitive the model is to kinetic parameter values that are not yet fully quantified. For example, the plots on the left side are for a case in which it is assumed that ferric iron reacts slowly relative to the H_2O_2 titration rate. The model predicts that, despite the presence of ferrous iron, the solution becomes saturated with respect to $UO_4 \bullet 2H_2O$. Ferric hydroxide is also predicted to precipitate once enough Fe(II) has been oxidized to Fe(III) by H_2O_2. However, if the rate of reaction of Fe(III) is a factor of seven times higher, the model predicts that the solution will reach steady-state concentrations of both H_2O_2 and Fe(III) that fall below precipitation thresholds (Figure 9, top left). The amount of O_2

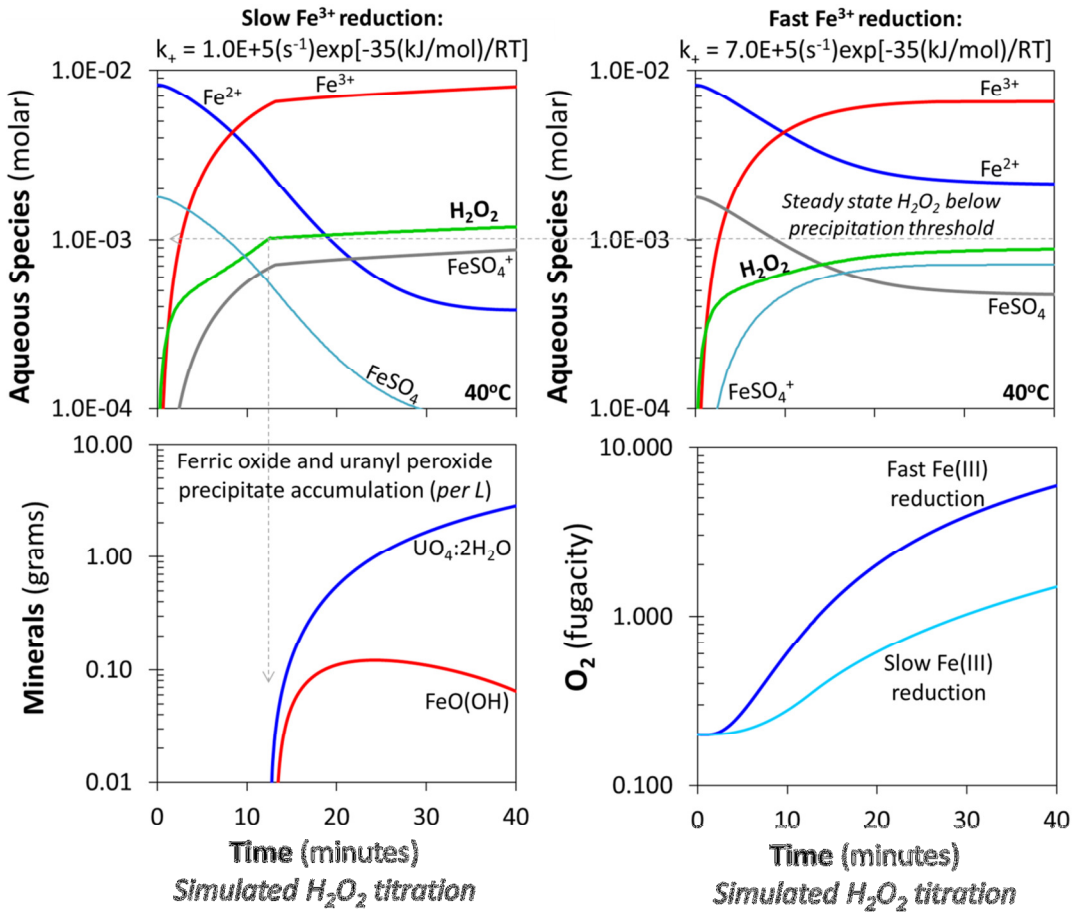

FIGURE 9 Results from the Thermodynamic/Kinetic Model Showing How the Interplay of Fe(II) Oxidation and the Rate of Fe(III) Reduction Determines the Steady-State Concentration of H_2O_2 for a Constant Titration Rate of 7 µmoles per Kilograms Solution per Second (110 g-U/L uranyl sulfate at pH = 1). These calculations show how the model can be used to determine the amount of ferrous and/or ferric iron needed to suppress uranyl peroxide precipitation.

released is also significantly affected by the Fe(III) reaction rate and may, therefore, represent an easily measurable quantity that can be used to constrain key reaction rates.

The model results also indicate that the formation of the stable ferrous sulfate complex, $FeSO_4$, needs to be taken into account in determining the amount of iron required to suppress $UO_4 \bullet 2H_2O$ precipitation.

3.3 VAN DE GRAAFF RESULTS

The first two irradiations performed at the Van de Graaff accelerator were done in pulse mode, with the temperature kept constant at 12°C and the average current at 5 μA. Because the pulse generator stopped working, the next set of irradiations was done in the DC mode. In all irradiations, the conversion factor from irradiation time in minutes to does in Mrad was 2.63 Mrad/μA-min. The RGA scanned the carrier gas stream approximately every 25 s.

In the first two irradiations, doses of 5,500 and 8,300 Mrad in the pulse mode were applied to the samples. In the second set of irradiations, doses between 11,700 and 32,500 Mrad in the DC mode were applied to the solutions. After precipitation did not occur in the uranyl sulfate solution containing 163 g-U/L and 70 ppm Fe in the DC mode (sample 3), a new solution containing 10 ppm Fe and 115 g-U/L was irradiated for all remaining tests. The concentration of peroxide in solution was measured by the method described in the experimental section (using toluidine blue) approximately 20 min after the end of irradiation. The concentration of peroxide in solution was also calculated by subtracting the number of micromoles of oxygen from one-half the number of micromoles of hydrogen. The two independent ways of measuring peroxide concentration in solution are significantly different. Using the gas analysis results as a means to determine the peroxide concentration in solution yields values 50-500 times greater than the values determined with the toluidine blue method. Using the gas analysis data to determine the amount of peroxide in solution does not take into account what will happen with direct effects on the sulfate and uranyl species. These effects might not be important at low concentrations, but at the concentrations in these experiments, at least 20% of the energy will be used in ionizing these species. The resulting ions could have all sorts of effects, including ejecting oxygen or acting as a sink for hydrogen. Therefore, the theoretical amount of hydrogen peroxide is likely an overestimation. Table 1 shows the results for seven irradiations. Table 2 shows the G values for hydrogen and oxygen, and these numbers are comparable to those obtained in 2012 [1].

3.3.1 Samples 1 and 2

For the first two samples, the starting uranium concentration was 163 g-U/L, and the Fe concentration was 70 ppm (most likely present as Fe^{3+}). No precipitation occurred during the first irradiation, where a dose of 5500 Mrad was applied to the solution, and the amount of peroxide in solution 20 min post-irradiation was 82 μM. In the second irradiation, a precipitate was observed, and 20 min after irradiation, the solution and precipitate were centrifuged. The solution was analyzed, and the concentration of peroxide was 39 μM. Based on ICP-OES results for uranium concentration before and after irradiation, 110 μmol uranyl peroxide was formed.

TABLE 1 Van de Graaff Irradiation Results for Uranyl Sulfate Solutions

Sample ID	Initial Uranium Concentration (g-U/L)	Final Uranium Concentration (g-U/L)	Dose (Mrad)	Mode	Peroxide Measured in Solution[a] (µmol)	Precipitate	Theoretical Peroxide[b] (µmol)	Solution Temperature (°C)	Total H_2 (µmol)	Total O_2 (µmol)	Final Ratio	Fe Concentration (ppm)
1	163	163	5500	Pulse	0.16	No	9.1	12	47.2	14.6	3.2	70
2	163	150	8300	Pulse	0.08	Yes	2.3	12	142	63	2.3	70
3	163	163	17900	DC	0.08	No	11.6	29	171	76	2.3	70
4	115	115	11700	DC	ND[c]	No	2.2	26	200	92	2.2	10
5	115	115	22400	DC	0.03	No	14.7	26	154	62	2.5	10
6	115	115	17700	DC	ND	No	18.1	34	243	103	2.4	10
7	115	115	32500	DC	0.03	No	15.1	34	595	282	2.1	10

[a] Determined by toluidine blue method.

[b] Determined by subtracting the number of micromoles of oxygen generated from one-half of the micromoles of hydrogen generated.

[c] Not detected.

The overall ratio of H_2 to O_2 generated in sample 1 was 3.2, and the gas analysis results as a function of dose are shown in Figures 10 and 11. The difference between these data and those reported earlier [1] is that the carrier gas was passed through the system once rather than being recycled. The µmoles of H_2 and O_2 reported here represent the amount in the He-gas stream that is passed over the irradiated solution, transported to the RGA for analysis, and disposed. The gas analysis had an approximately 20-min delay due to the time from sample generation to RGA analysis. The µmoles of each gas were calculated from the flow rate of the carrier gas and the percent H_2 and O_2 in the sample. The total µmoles of each gas produced was calculated by summing the µmoles found in each sample. Figures 12 and 13 show the gas analysis results for sample 2, where larger amounts of H_2 and O_2 were produced due to a higher dose being applied to the sample. The gas analysis data for both samples (Figures 10 and 12) show that the generation of hydrogen and oxygen continues to increase with dose. The few dips in the curves are possibly due to fluctuations in power.

TABLE 2 G Values for Hydrogen and Oxygen

Sample ID	G (molecules/100 eV)	
	H_2	O_2
1	0.041	0.013
2	0.087	0.038
3	0.046	0.020
4	0.083	0.038
5	0.033	0.013
6	0.066	0.028
7	0.088	0.042

3.3.2 Sample 3

Due to the failure of the pulse generator, sample 3 was irradiated in the DC mode at the same average current. The temperature of the sample was warmer at 29°C compared to the samples irradiated in pulse mode, which were kept at 12°C, but the dose applied to the sample was more than double the dose applied to sample 2. Precipitation did not occur, and the overall H_2-to-O_2 ratio was 2.3. The peroxide concentration in solution was 39 µM, and the amounts of hydrogen and oxygen produced were only slighter more than the amounts produced in sample 2, despite the dose applied to sample 3 being more than two times larger than the dose applied to sample 2. Figures 14 and 15 show the gas analysis data for sample 3.

3.3.3 Samples 4-7

Because precipitation could not be achieved in the DC mode with the sample containing 70 ppm Fe, a new uranyl sulfate solution was used for samples 4-7. The solution contained 115 g-U/L and 10 ppm Fe. Samples 4 and 5 were kept at 26°C, and samples 6 and 7 were kept at 34°C. Doses applied to the solutions ranged from 11,700 to 32,500 Mrad. Peroxide could not be measured by the toluidine blue method for samples 4 and 6, and the peroxide concentrations measured for samples 5 and 7 were 12.8 µM and 16.5 µM, respectively. Precipitation did not occur in samples 4-7, and the overall H_2-to-O_2 ratio ranged from 2.1 to 2.5. Figures 16-23 show the gas-analysis data collected for samples 4-7. The peaks and valleys in the gas analysis data could be due to power fluctuations during each irradiation. One of the improvements that will be made to the system during future irradiations will be a continuous monitor for the power being applied to the sample.

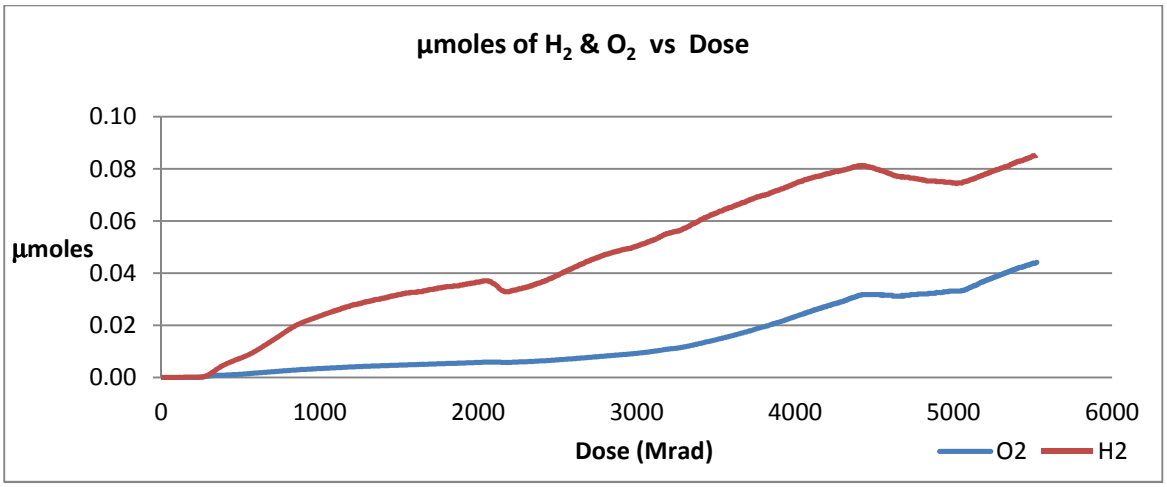

FIGURE 10 H_2 and O_2 Produced as a Function of Dose for Sample 1

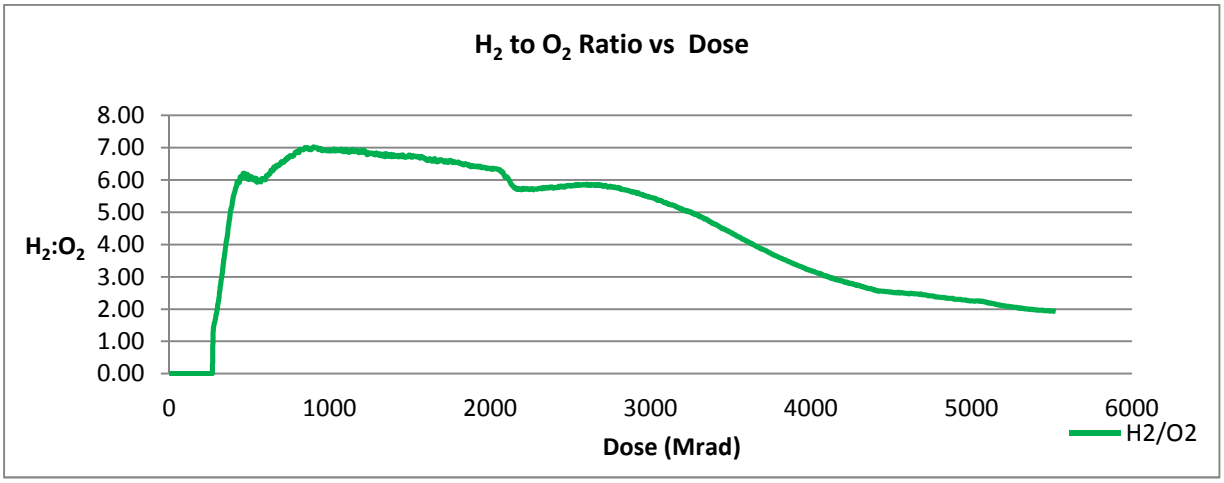

FIGURE 11 H_2-to-O_2 Ratio as a Function of Dose for Sample 1

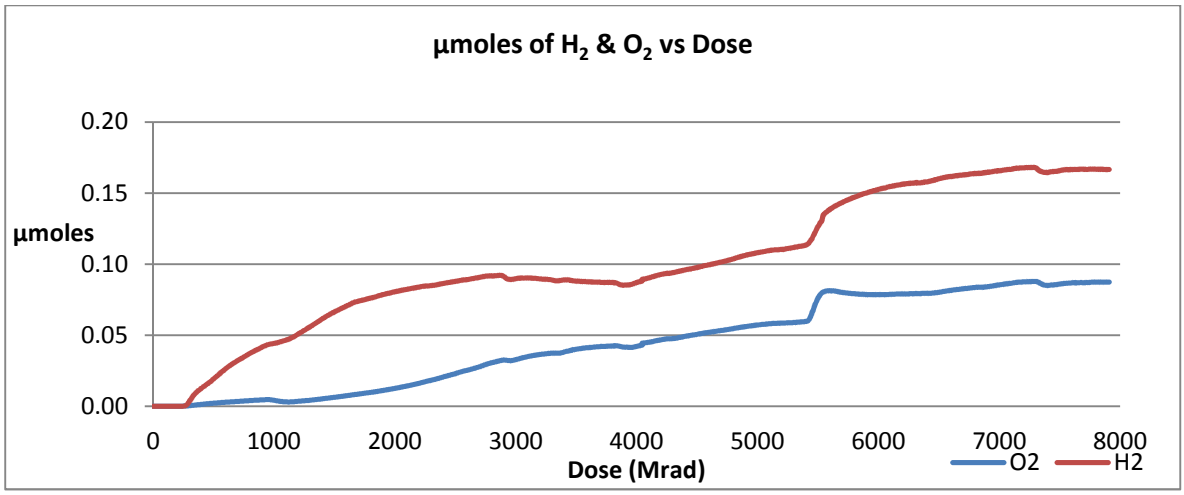

FIGURE 12 H_2 and O_2 Produced as a Function of Dose for Sample 2

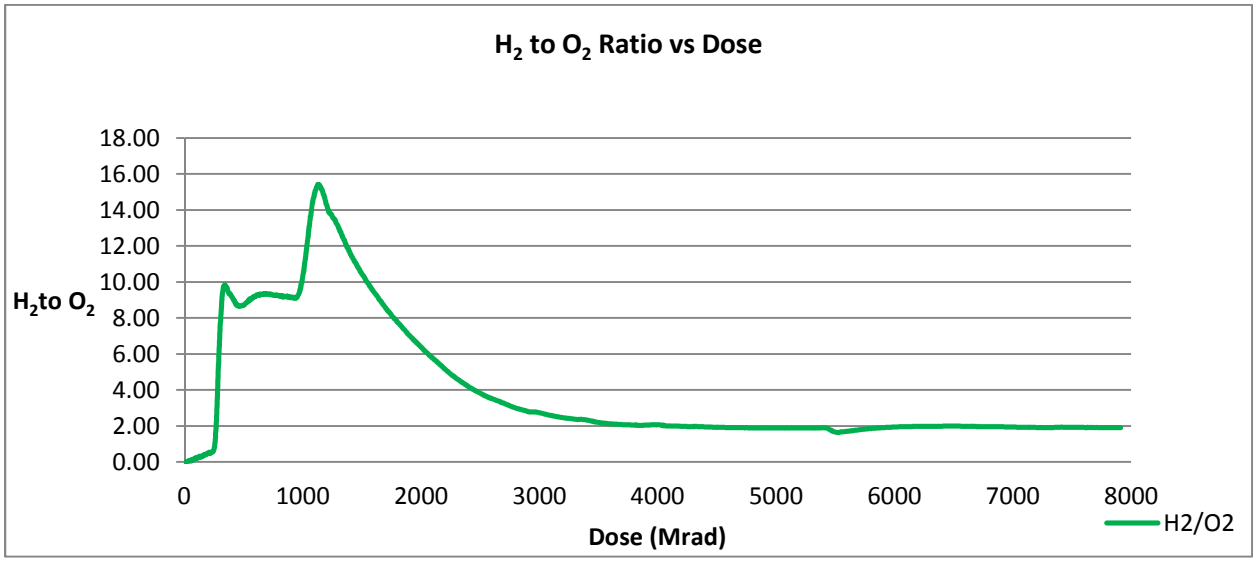

FIGURE 13 H_2-to-O_2 Ratio as a Function of Dose for Sample 2

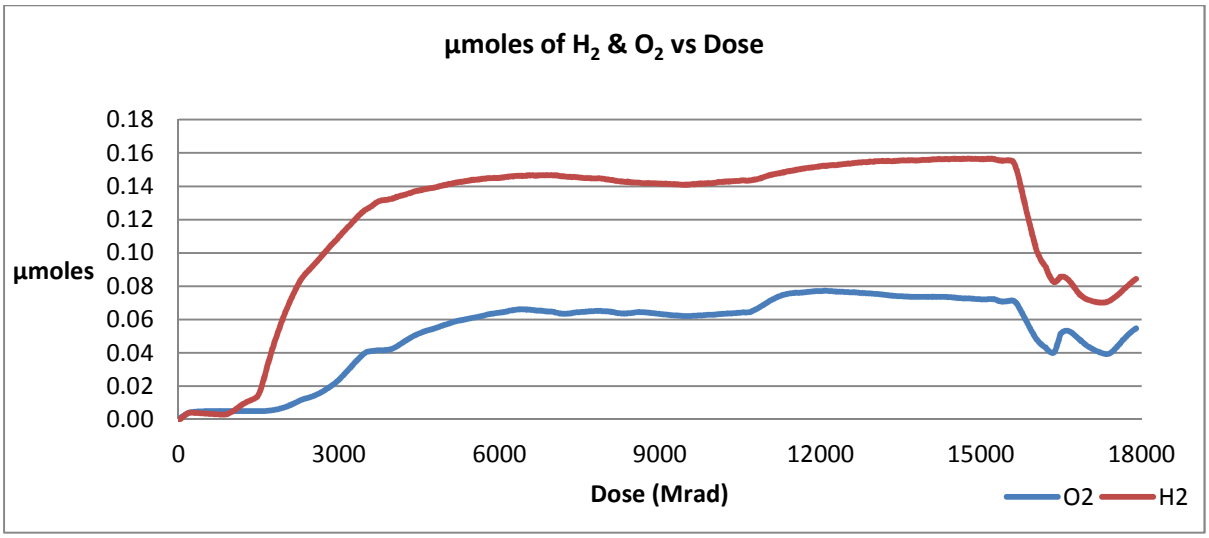

FIGURE 14 H_2 and O_2 Produced as a Function of Dose for Sample 3

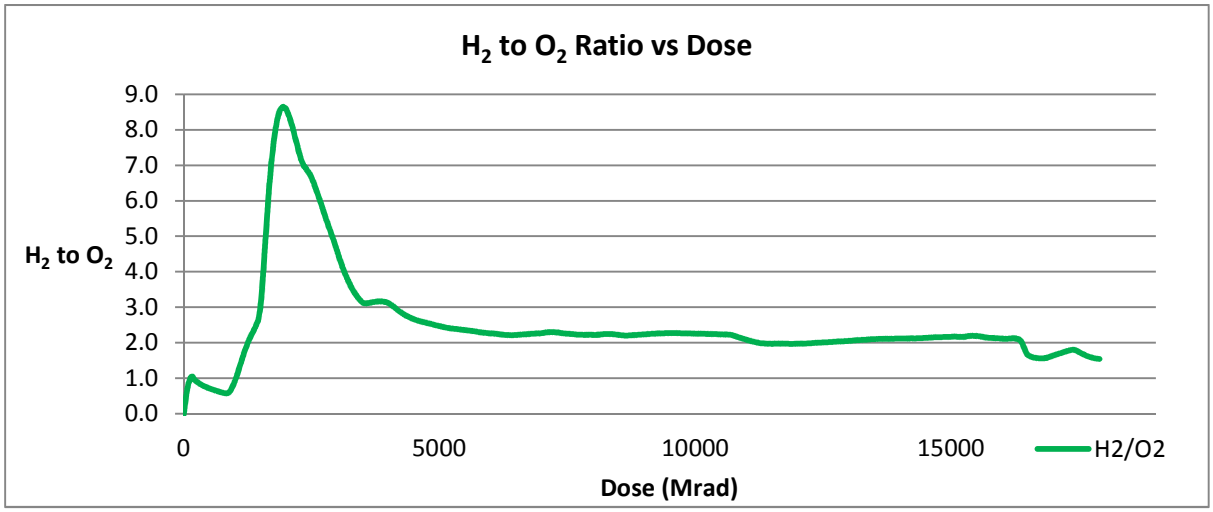

FIGURE 15 H_2-to-O_2 Ratio as a Function of Dose for Sample 3

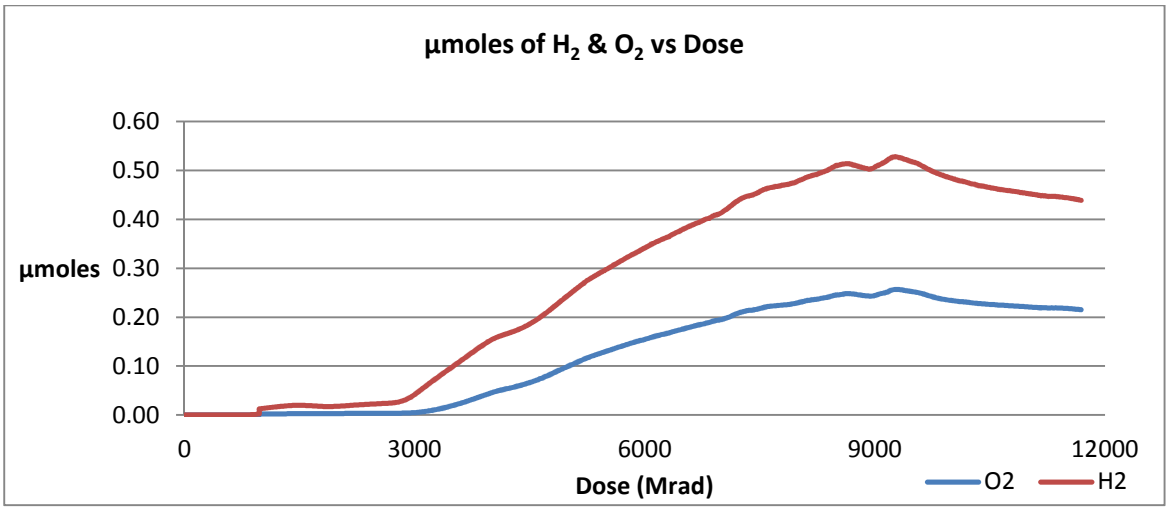

FIGURE 16 H_2 and O_2 Produced as a Function of Dose for Sample 4

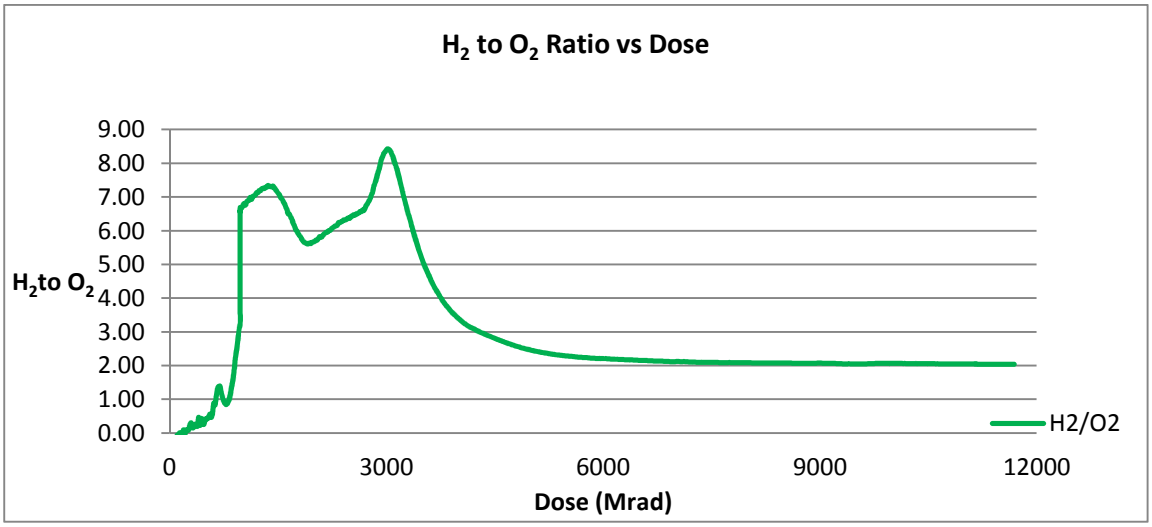

FIGURE 17 H_2-to-O_2 Ratio as a Function of Dose for Sample 4

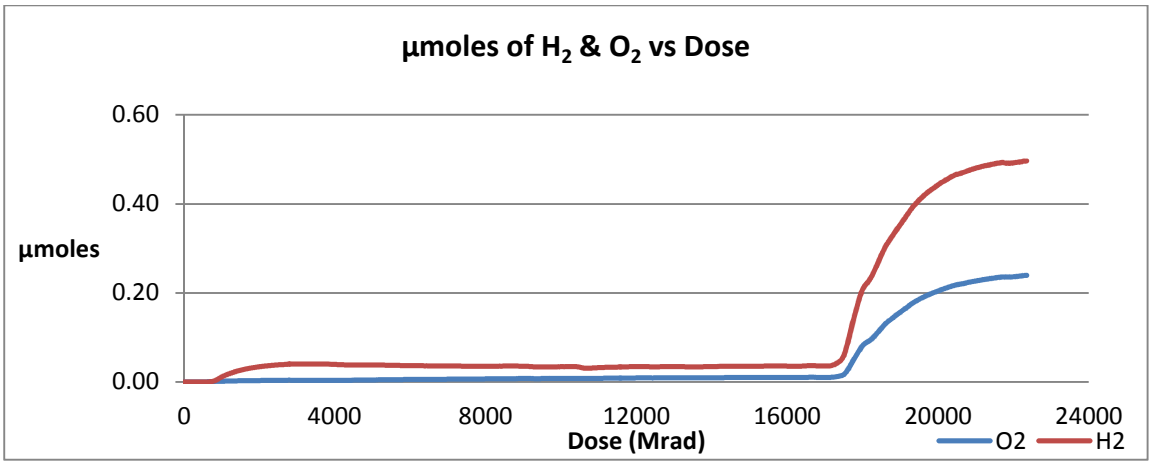

FIGURE 18 H_2 and O_2 Produced as a Function of Dose for Sample 5

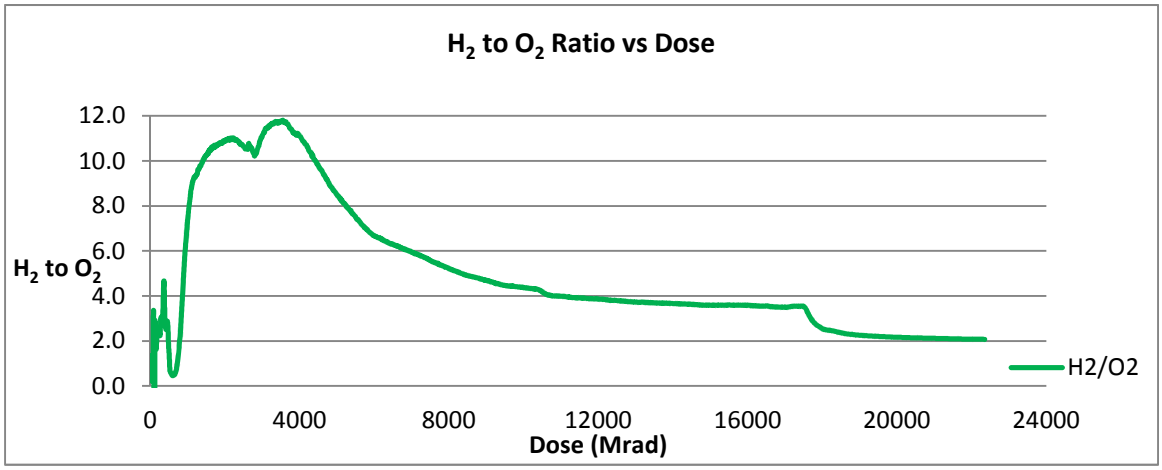

FIGURE 19 H_2-to-O_2 Ratio as a Function of Dose for Sample 5

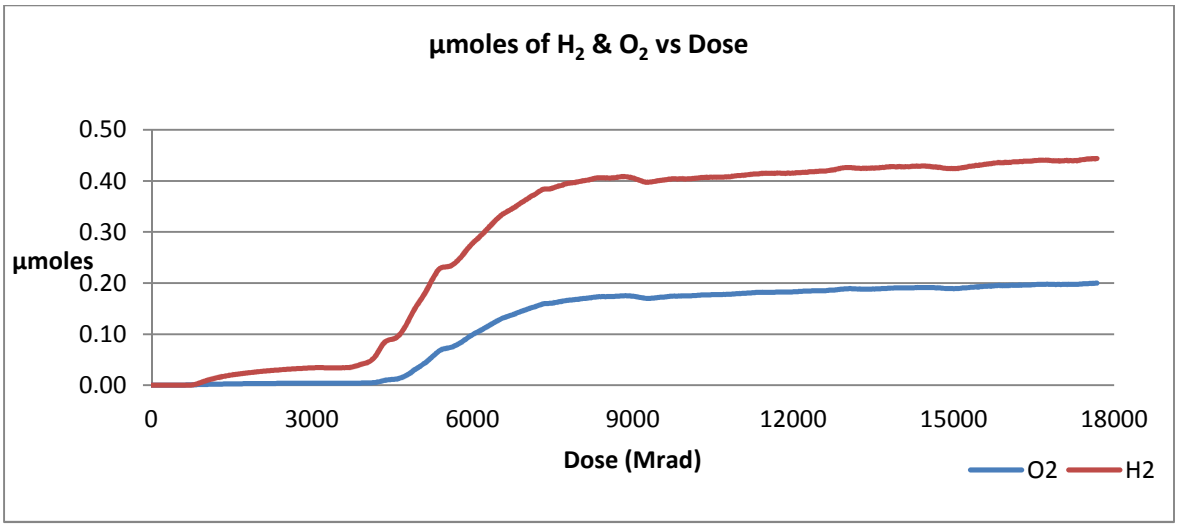

FIGURE 20 H_2 and O_2 Produced as a Function of Dose for Sample 6

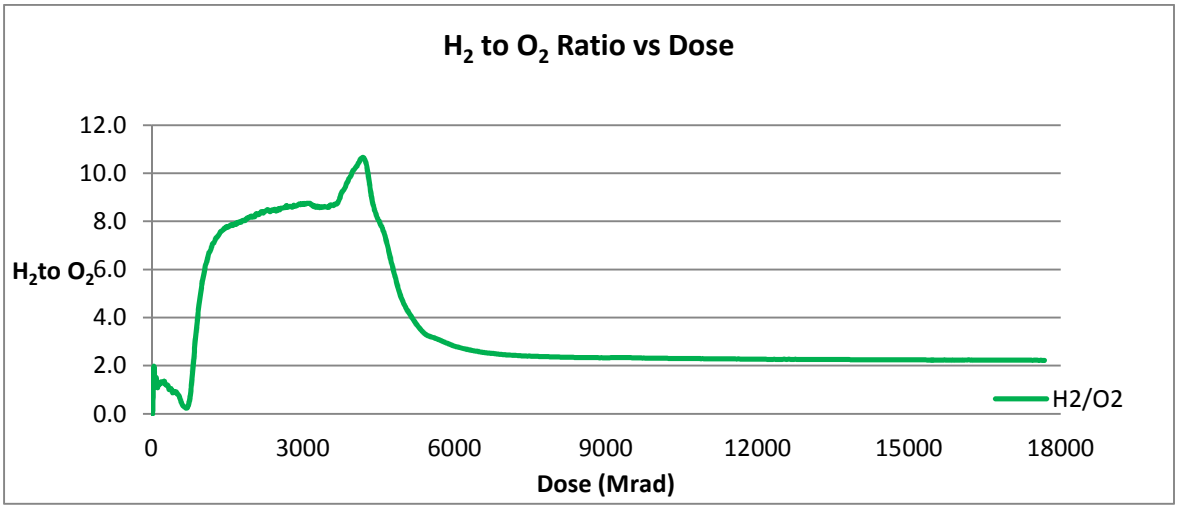

FIGURE 21 H_2-to-O_2 Ratio as a Function of Dose for Sample 6

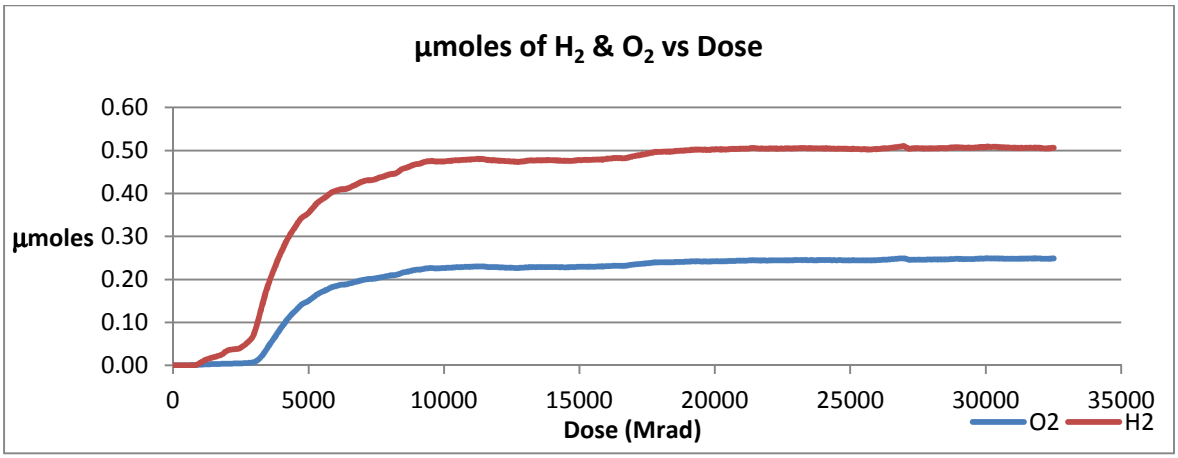

FIGURE 22 H_2 and O_2 Produced as a Function of Dose for Sample 7

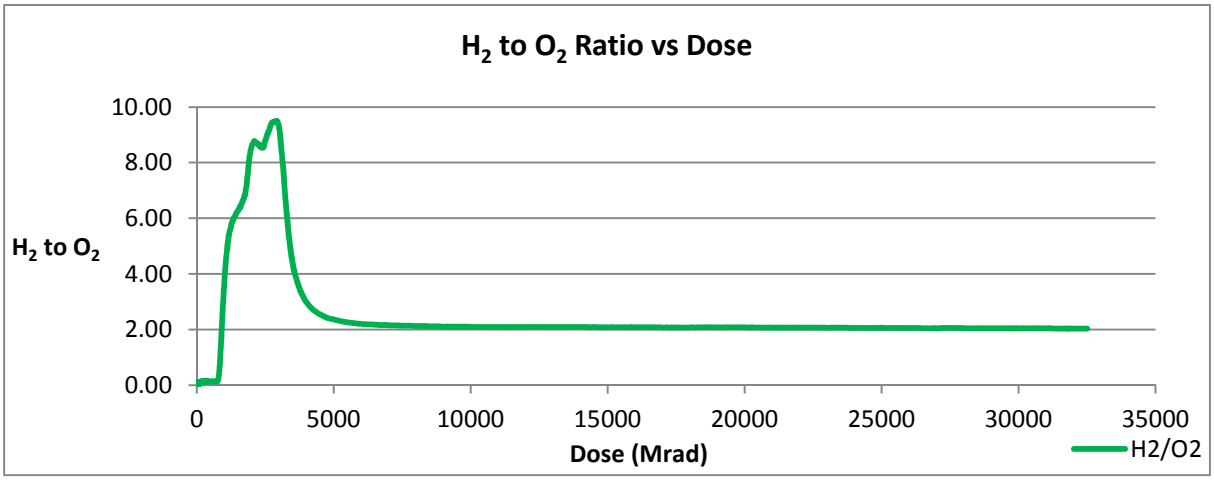

FIGURE 23 H_2-to-O_2 Ratio as a Function of Dose for Sample 7

4 CONCLUSIONS

Even without dissolved salts and gases in solution, it has been shown that 50 elementary reactions and their rate constants are required to adequately describe radiolysis of water and its subsequent relaxation [10]. Further complications are added by dissolved species (gases and salts), which can react with hydrated electrons, radicals, intermediates, and molecular species; these reactions affect both the generation rate of hydrogen and hydrogen peroxide and the decomposition of hydrogen peroxide. Hydrogen peroxide can be oxidized to oxygen, reduced to water, or self-destruct into water and oxygen [10]. Another complication is that such high concentrations of solutes will deposit considerable energy in the solution.

All these factors lead to a complicated experimental system that must be understood to predict the steady-state concentration of peroxide in the SHINE target solution during operating conditions and avoid precipitation of uranyl peroxide. The work that has been performed thus far provides some insights into the system, but more work is certainly required and is planned.

4.1 BENCH-TOP EXPERIMENTS

The following observations were made from the bench-top titration experiments with a 110 g-U/L uranyl sulfate solution and hydrogen peroxide:

- The solubility product for the uranyl peroxide precipitate determined by titration (K_{sp} = 0.0021, log K_{sp} = -2.673) at 25°C agrees with the solubility product recently measured by an undersaturation approach [8].

- The precipitate formed in the titration solubility tests was confirmed by XRD to be crystalline metastudtite (UO_4•$2H_2O$). No other mineral phases were detected.

- The solubility of UO_4•$2H_2O$ is strongly temperature dependent. Based on experimental results, the solubility product increases from around 0.0021 (log K_{sp} = -2.673) at 25°C to 0.01 (log K_{sp} = -1.850) at 60°C.

The titration method was also used to determine the effectiveness of ferric and ferrous iron as reagents for the decomposition of peroxide in 110 g-U/L uranyl sulfate at pH 1. The following conclusions were made:

- The reduction of H_2O_2 by ferrous iron is more rapid than the oxidation of H_2O_2 by ferric iron under relevant experimental conditions.

- The amount of ferrous iron needed to establish a H_2O_2 steady-state concentration below the uranyl peroxide precipitation threshold was determined for a given set of relevant experimental conditions.

Based on the experimental results and relevant literature, a thermodynamic/kinetic model for the precipitation of uranyl peroxide for a given set of relevant conditions was developed and tested. The relevant conditions that must be specified in the model are the temperature, the uranyl sulfate concentration, the iron concentration, and the H_2O_2 production rate.

4.2 MODEL DEVELOPMENT

The purpose of the model is to:

- Provide a predictive tool for calculating the amount of iron required to avoid uranyl peroxide precipitation.
- Provide a quantitative description of the kinetic processes involved in the decomposition of hydrogen peroxide under relevant conditions.

The model was found to work as intended and thus represents a useful tool for calculating the steady-state concentrations or activities of species resulting from a set of interacting kinetic reactions. The applicability of the model to understanding the catalytic decomposition of hydrogen peroxide to avoid uranyl peroxide precipitation will depend on whether the relevant kinetic data needed to calibrate the model can be found in the literature or determined experimentally.

4.3 VAN DE GRAAFF EXPERIMENTS

The planned experiments to study the effects of temperature and power on uranyl peroxide precipitation could not be performed because precipitation could not be repeated in the DC mode. As a result, several changes will be made to the system components to be able to understand the effects of temperature and power on precipitation formation. The three main changes include using a uranyl sulfate solution that does not contain Fe, monitoring the gas flow rates continuously, and measuring the power applied to the sample continuously. A big difference between this set of experiments and the experiments performed in 2012 is that both solutions tested recently contained Fe, while the solutions tested in 2012 were never analyzed for Fe. The pulse generator has also been repaired because, as seen from the current set of results, precipitation is more likely to occur in the pulse than the DC mode.

Precipitation did occur in the pulse but not in the DC mode. In the pulse mode, a set of reactions occurs that does not occur in the DC mode. Reactions induced by radiation in water consist of three different types: (1) reactions in the initial energy deposition region (the “spur”), (2) reactions between “spurs,” and (3) reactions between radiation-induced species and material in the bulk of the solution. In DC mode radiolysis, type two reactions are almost completely eliminated. If reactions between “spurs” lead to localized concentrations that are higher than those in the bulk, precipitation is likely to occur. If the dissolution reaction rate is very low, this could lead to precipitation in the pulsed but not in the DC mode.

5 REFERENCES

[1] Kalensky, M., Chemerisov, S., Youker, A., Tkac, P., Krebs, J., Quigley, K., Lowers, R., Bakel, A., and Vandegrift, G. F., *Means to Eliminate Uranyl Peroxide Precipitation in SHINE Target Solution*, Argonne National Laboratory Report ANL/CSE-13/21 (2013).

[2] Silverman, M.D., Watson, G.M., and McDuffie, H.F., "Peroxide Decomposition in Aqueous Homogeneous Reactor Fuels," *Ind. Eng. Chem.* **48**(8): 1238-1241 (1956).

[3] Silverman, L., Sallach, R., Seitz, R., and Bradshaw, W., "Catalytic Decomposition of Hydrogen Peroxide and Uranyl Peroxide," *Ind. Eng. Chem.* **50**(12): 1785-1786 (1958).

[4] Bibler, N., "Radiolysis of 0.4 M Sulfuric Acid Solutions with Fission Fragments from Dissolved Californium-252: Estimated Yields of Radical and Molecular Products that Escape Reactions in Fission Fragment Tracks," *J. Phys. Chem.* **79**(19): 1991-1995 (1975).

[5] Draganic, I., "Oxalic Acid: The Only Aqueous Dosimeter for In-Pile Use," *Nucleonics* **21**(2): 33 (1963).

[6] Sunil, K., and Narayana, B., "Spectrophotometric Determination of Hydrogen Peroxide in Water and Cream Samples," *Bull. Environ. Contam. Toxicol.* **81**: 422-426 (2008).

[7] Wolery, T.J., and Jove-Colon, C.F., "Qualification of Thermodynamic Data for Geochemical Modeling of Mineral–Water Interactions in Dilute Systems," Prepared for U.S. Department of Energy Office of Civilian Radioactive Waste Management Office of Repository Development, ANL-WIS-GS-000003 REV 01 (June 2007).

[8] Giménez, J., de Pablo, J., Casas, I., Martínez-Lladó, X., Rovira, M., and Martínez Torrents, A., "Solubility Study and Point of Zero Charge of Studtite (UO_2O_2:$4H_2O$)," *Appl. Geochem.* **49**: 42–45 (2014).

[9] Stumm, W., and Lee, G. F., "Oxygenation of Ferrous Iron," *Ind. Eng. Chem.* **53**: 143 (1961).

[10] Wren, J.C., "Steady-State Radiolysis: Effects of Dissolved Additives," Chapter 22, *Nuclear Energy and the Environment*, ACS Symposium Series 1046, eds., Chien M. Wei and Bruce J. Mincher, American Chemical Society, Washington D.C. (2010).

Chemical Sciences and Engineering Division
Argonne National Laboratory
9700 South Cass Avenue, Bldg. 205
Argonne, IL 60439-4837

www.anl.gov

Argonne National Laboratory is a U.S. Department of Energy
laboratory managed by UChicago Argonne, LLC